Mass of the b quark and B -meson decay constants from Nf=2+1+1 twisted-mass lattice QCD

Bussone, A.; Carrasco, N.; Dimopoulos, P; Frezzotti, R.; Lami, P.; Lubicz, Vittorio; Picca, E.; Riggio, L.; Rossi, G. C.; Simula, Silvano; Tarantino, C.; ETM Collaboration

Published in:
Physical Review D

DOI:
10.1103/PhysRevD.93.114505

Publication date:
2016

Document version:
Final published version

Mass of the b quark and B-meson decay constants from $N_f = 2 + 1 + 1$ twisted-mass lattice QCD

A. Bussone,[1] N. Carrasco,[2] P. Dimopoulos,[3,4,*] R. Frezzotti,[4,5] P. Lami,[6] V. Lubicz,[2,6] E. Picca,[6] L. Riggio,[2] G. C. Rossi,[3,4,5] S. Simula,[2] and C. Tarantino[6,2]

(ETM Collaboration)

[1]*CP3-Origins & Danish IAS, University of Southern Denmark, Campusvej 55, 5230 Odense, Denmark*
[2]*INFN, Sezione di Roma Tre, Via della Vasca Navale 84, I-00146 Rome, Italy*
[3]*Centro Fermi—Museo Storico della Fisica e Centro Studi e Ricerche Enrico Fermi, Compendio del Viminale, Piazza del Viminiale 1, I-00184 Rome, Italy*
[4]*Dipartimento di Fisica, Università di Roma "Tor Vergata", Via della Ricerca Scientifica 1, I-00133 Rome, Italy*
[5]*INFN, Sezione di "Tor Vergata", Via della Ricerca Scientifica 1, I-00133 Rome, Italy*
[6]*Dipartimento di Fisica, Università Roma Tre, Via della Vasca Navale 84, I-00146 Rome, Italy*

(Received 23 March 2016; published 7 June 2016)

We present precise lattice computations for the b-quark mass, the quark mass ratios m_b/m_c and m_b/m_s as well as the leptonic B-decay constants. We employ gauge configurations with four dynamical quark flavors, up-down, strange and charm, at three values of the lattice spacing ($a \sim 0.06$–0.09 fm) and for pion masses as low as 210 MeV. Interpolation in the heavy quark mass to the bottom quark point is performed using ratios of physical quantities computed at nearby quark masses exploiting the fact that these ratios are exactly known in the static quark mass limit. Our results are also extrapolated to the physical pion mass and to the continuum limit and read $m_b(\overline{\mathrm{MS}}, m_b) = 4.26(10)$ GeV, $m_b/m_c = 4.42(8)$, $m_b/m_s = 51.4(1.4)$, $f_{Bs} = 229(5)$ MeV, $f_B = 193(6)$ MeV, $f_{Bs}/f_B = 1.184(25)$ and $(f_{Bs}/f_B)/(f_K/f_\pi) = 0.997(17)$.

DOI: 10.1103/PhysRevD.93.114505

I. INTRODUCTION

Lattice QCD simulations constitute the current dominant theoretical framework for high-precision B-physics computations which are necessary, in combination with experimental results, to obtain precious information in the quark sector phenomenology. In fact, increasingly improved computations of matrix elements (decay constants, form factors and mixing parameters) are of high importance to carry out challenging tests of the Cabibbo-Kobayashi-Maskawa (CKM) paradigm, an effort also stimulated by the ambitious prospect of discovering footprints of new physics effects. Moreover, lattice methods are optimal to determine the quark masses by confronting experimental quantities from spectroscopy with their theoretical counterparts computed from first principles via lattice QCD simulations.

We should stress that although direct lattice simulations are not yet possible at the physical value of the b-quark mass due to computing power limitations, the combined use of effective theories and improved lattice techniques has progressively led to results that are characterized by much reduced and reliable systematic uncertainties.

In the present paper, we have carried out a nonperturbative determination of the b-quark mass as well as its ratios to the charm and the strange quark mass. The latter turn out to be very accurate because the renormalization scheme dependence is absent and the systematics related to the lattice scale determination are suppressed. We observe that a precise b-quark mass evaluation is important for reducing the uncertainty in the study of Higgs decays to $b\bar{b}$ [1] and possibly unveil non-SM features of the $H - b - \bar{b}$ coupling.

In this paper, we have also computed the pseudoscalar B-decay constants f_{Bs} and f_B as well as their (SU(3)-breaking) ratio, f_{Bs}/f_B. Currently there is high experimental interest by LHCb and B factories in the processes $B_{(s)} \to \mu^+\mu^-$ [2] and $B \to \tau\nu$ [3,4] for the full description of which the knowledge of the aforementioned decay constants is indispensable. The importance of B-decays is not limited only to their crucial contribution for improving the accuracy of the unitarity triangle determination; in fact B-decays in channels that are loop suppressed in SM are some of the first-class candidates for revealing features of beyond the Standard Model (SM) dynamics.

In our lattice computation, we have used $N_f = 2+1+1$ dynamical quark gauge configurations generated by ETM Collaboration [5,6] at three values of the lattice spacing. Our results are extrapolated to the continuum limit. For the determination of the B-physics observables, we have employed the ETMC ratio method that has already been applied within the $N_f = 2$ lattice simulations framework

*Corresponding author.
dimopoulos@roma2.infn.it

[7–9]. In particular, in the present paper, we have brought about improvements of the ratio method implementation thanks to which it is possible to gain better control of various sources of systematic uncertainty.

The plan of the paper is as follows. We describe our computational setup in Sec. II. In Sec. III, we present an improved implementation of the ratio method in the cases of the determination of the b-quark mass, its ratios to the charm and strange quark masses, and the pseudoscalar B-decay constants. We also give a detailed error budget for each one of the observables studied in the present work. Finally, in Sec. IV, we compare our results with the ones provided by other lattice collaborations. For the interested reader, recent reviews on B-physics lattice computational methods, techniques and collection of results are given in Refs. [10–13]. Recent nonlattice results can be found e.g. in Refs. [14–16].

II. COMPUTATIONAL DETAILS

A. Lattice action setup

In our computation, we employ Iwasaki glue [17,18] and a mixed lattice fermionic action setup. The sea quark action for the light mass-degenerate sea quark doublet, S_ℓ, and the action for the strange and charm quark doublet, S_h ([19,20]) read, respectively,

$$S_\ell^{\rm sea} = a^4 \sum_x \bar{\psi}_\ell(x) \left\{ \frac{1}{2}\gamma_\mu(\nabla_\mu + \nabla_\mu^*) - i\gamma_5\tau^3 \times \left[M_{\rm cr} - \frac{a}{2}\sum_\mu \nabla_\mu^*\nabla_\mu \right] + \mu_\ell \right\} \psi_\ell(x), \quad (1)$$

$$S_h^{\rm sea} = a^4 \sum_x \bar{\psi}_h(x) \left\{ \frac{1}{2}\gamma_\mu(\nabla_\mu + \nabla_\mu^*) - i\gamma_5\tau^1 \times \left[M_{\rm cr} - \frac{a}{2}\sum_\mu \nabla_\mu^*\nabla_\mu \right] + \mu_\sigma + \mu_\delta\tau^3 \right\} \psi_h(x), \quad (2)$$

where ∇_μ and ∇_μ^* represent the nearest neighbor forward and backward covariant derivatives and it is intended that the untwisted mass has been tuned to its critical value, $M_{\rm cr}$. In Eq. (1), we have defined the quark doublet $\psi_\ell = (\psi_u \psi_d)^T$ while μ_ℓ denotes the light (sea) twisted quark mass. In Eq. (2), $\psi_h = (\psi_s, \psi_c)^T$ denotes the strange-charm fermion doublet while μ_σ and μ_δ are the bare twisted mass parameters from which the renormalized (sea) strange and charm masses can be derived. Pauli matrices in Eqs. (1) and (2) act in flavor space. For more details on the twisted mass setup, we refer the reader to Refs. [5,6,19–23].

In the valence sector, we employ the Osterwalder-Seiler (OS) action [24] which is written as the sum of individual quark flavor contributions,

$$S_q^{\rm val,OS} = a^4 \sum_x \sum_f \bar{q}_f \left\{ \frac{1}{2}\gamma_\mu(\nabla_\mu + \nabla_\mu^*) - i\gamma_5 r_f \left[M_{\rm cr} - \frac{a}{2}\sum_\mu \nabla_\mu^*\nabla_\mu \right] + \mu_f \right\} q_f(x), \quad (3)$$

where the label f runs over the different valence flavors—light, strange, charm or heavier and $r_f = \pm 1$. Valence and sea quark masses are matched to each other and fixed in terms of meson masses in order to ensure unitarity in the continuum limit. Lattice artifacts in physical observables are just $O(a^2)$ [19,25].

B. Simulation parameters and correlation functions

We have used the $N_f = 2 + 1 + 1$ gauge ensembles generated by the ETM Collaboration [5,6]. A summary of the most important details of our simulations is given in Table I.

Simulation data have been taken at three values of the lattice spacing, namely $a = 0.0885(36)$, $0.0815(30)$ and $0.0619(18)$ fm, corresponding to $\beta = 1.90$, 1.95 and 2.10, respectively (see Ref. [26]). In our simulation, the light valence and sea quark masses are set equal, leading to pion masses in the range between 210 and 450 MeV. Strange and charm sea quark masses are chosen close to their physical value and fixed from M_K and M_{D_s} inputs (see Ref. [26]). To allow for a smooth interpolation to the physical values of the valence strange and charm mass as well as for heavier quark masses, we have inverted the heavy valence Dirac matrix for three values of the strangelike quark mass, μ_s, and a number of charmlike and heavier quark mass, $a\mu_c - a\mu_h$.

We have fixed the lattice scale using f_π. The u/d, strange and charm quark masses have been determined comparing lattice data with the experimental values of the pion, K and $D_{(s)}$ meson mass, respectively. Further details can be found in Ref. [26]. The use of the mixed action of twisted mass and OS quarks offers the advantage that the masses of light quarks in the sea and of all types of quarks in the valence are multiplicatively renormalized via the renormalization constant (RC) $Z_m = 1/Z_P$. The latter is computed non-perturbatively using the RI -MOM scheme (for the RC determination, see Appendix A of Ref. [26]). Moreover, exact chiral lattice Ward-Takahashi identities imply that at maximal twisted angle no normalization constant is needed in the computation of decay constants [19,27].

In two-fermion correlation functions, valence light and strangelike quark propagators have been calculated with the "one-end" trick stochastic method [28,29] by employing spatial stochastic sources at a randomly chosen time slice. However for propagators of the charm or heavier quark, in order to get suppressed contribution of the excited states in the correlation functions, we have employed Gaussian smeared interpolating quark fields [30]. For the values of the smearing parameters, we set $k_G = 4$ and $N_G = 30$. In

TABLE I. Summary of simulation details. Gauge couplings $\beta = 1.90$, 1.95 and 2.10 correspond to lattice spacings $a \simeq 0.089$, 0.082 and 0.062 fm, respectively. We denote with $a\mu_\ell$, $a\mu_s$ and $a\mu_c - a\mu_h$, the light, strangelike, charmlike and heavier bare quark masses, respectively, entering in the valence sector computations. N_{cfg} stands for the number of gauge configurations used in the analysis.

β	V/a^4	$a\mu_{\rm sea} = a\mu_\ell$	N_{cfg}	$a\mu_s$	$a\mu_c - a\mu_h$
1.90	$32^3 \times 64$	0.0030	150	0.0180,	0.212 56, 0.250 00,
		0.0040	150	0.0220,	0.294 04, 0.345 83,
		0.0050	150	0.0260	0.406 75, 0.478 40,
					0.562 67, 0.661 78,
					0.778 36, 0.915 46
1.90	$24^3 \times 48$	0.0040	150		
		0.0060	150		
		0.0080	150		
		0.0100	150		
1.95	$32^3 \times 64$	0.0025	150	0.0155,	0.187 05, 0.220 00,
		0.0035	150	0.0190,	0.258 75, 0.304 33,
		0.0055	150	0.0225	0.357 94, 0.420 99,
		0.0075	150		0.495 15, 0.582 37
					0.684 95, 0.805 61
1.95	$24^3 \times 48$	0.0085	150		
2.10	$48^3 \times 96$	0.0015	90	0.0123,	0.144 54, 0.170 00,
		0.0020	90	0.0150,	0.199 95, 0.235 17,
		0.0030	90	0.0177	0.276 59, 0.325 31,
					0.382 62, 0.450 01,
					0.529 28, 0.622 52

addition, we apply APE-smearing to the gauge links [31] in the interpolating fields with parameters $\alpha_{\rm APE} = 0.5$ and $N_{\rm APE} = 20$. Smearing leads to improved projection onto the lowest energy eigenstate at small Euclidean time separations. We have implemented smeared fields in both source and sink. We have thus evaluated two-point heavy-light correlation functions made up by the four possible combinations of local-smeared source-sink. We can thus employ the GEVP method [32] to compute the ground state pseudoscalar masses. For the pseudoscalar decay constant calculation, we evaluate two-point correlation functions with pseudoscalar interpolating operators $P(x) = \bar{q}_1(x)\gamma_5 q_2(x)$. The typical form of the correlation function and its asymptotic behavior on periodic lattices read

$$C_{PP}(t) = (1/L^3)\sum_{\vec{x}} \langle P(\vec{x},t)P^\dagger(\vec{0},0)\rangle \xrightarrow{t\gg 0,(T-t)\gg 0} \times \frac{\xi_{PP}}{2M_{ps}}(e^{-M_{ps}t} + e^{-M_{ps}(T-t)}). \quad (4)$$

We set opposite Wilson parameters, r_f, for the two valence quarks that form the pseudoscalar meson. This choice guarantees that the cutoff effects on the pseudoscalar mass are $O(a^2\mu_q)$ [19,33,34]. We consider two cases, using smeared source only and source and sink both smeared, for which ξ_{PP} is given by $\xi_{PP} = \langle 0|P^L|ps\rangle\langle ps|P^S|0\rangle$ in the first case and $\xi_{PP} = \langle 0|P^S|ps\rangle\langle ps|P^S|0\rangle$ in the second one, where L and S indicate local and smeared operators, respectively. From the combination of the two kinds of correlators it is easy to get the matrix element of the local operator, namely, $g_{ps} = \langle 0|P^L|ps\rangle$ which, via PCAC, allows for the computation of the pseudoscalar decay constant:

$$f_{ps} = (\mu_1 + \mu_2)\frac{g_{ps}}{M_{ps}\sinh M_{ps}}, \quad (5)$$

where $\mu_{1,2}$ are the masses of the valence quarks entering the pseudoscalar meson mass M_{ps}. In Eq. (5), the use of $\sinh M_{ps}$ rather than M_{ps} turns out to be advantageous for getting reduced discretization errors. In Fig. 1, we illustrate the beneficial effect of smearing in determining the ground state signal at early time distance and making possible the decay constant evaluation for values of the heavy quark mass for which it fails if local interpolating fields only are used. In the figure, we show the results at $\beta = 1.95$ and $a\mu_{\rm sea} = a\mu_\ell = 0.0035$ obtained for the heavy-light effective mass versus the Euclidean time separation panel (a) and the decay constant versus the heavy quark mass panel (b) using either only local or appropriate combinations of local and smeared interpolating fields.

For each of the $\beta = 1.90$ and 1.95 gauge ensembles, the ETM Collaboration has produced around 5000 thermalized trajectories. For the ensembles at $\beta = 2.10$ corresponding to the two heaviest light quark masses (i.e. $a\mu_{\rm sea} = 0.0020$, 0.0030), 4000 trajectories have been generated; while for the case of the lightest sea quark mass ($a\mu_{\rm sea} = 0.0015$), the total number of the generated trajectories is about 2100. All

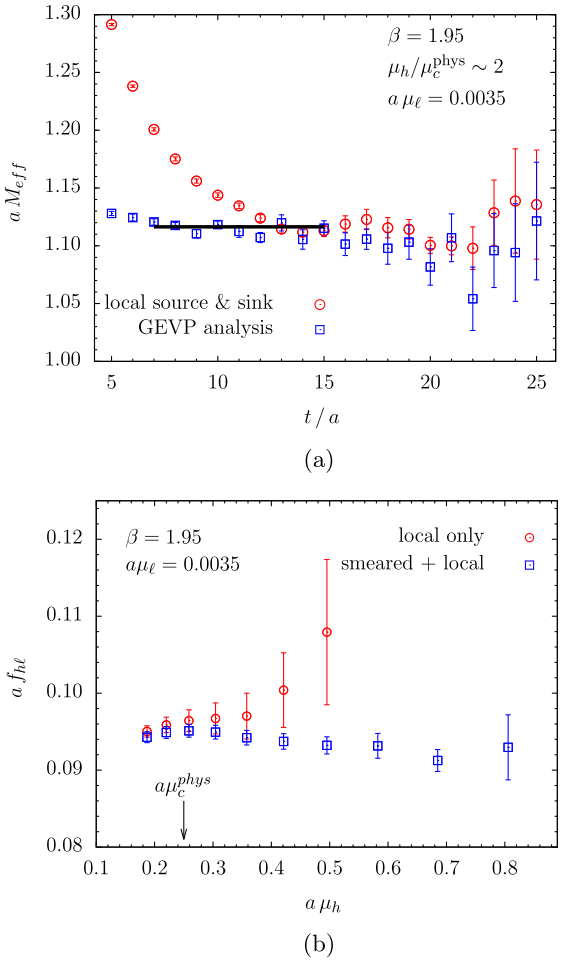

FIG. 1. (a) Effective mass of the pseudoscalar 2-point correlator obtained using either a local source and sink (red circles) or the GEVP method (blue squares) applied to a matrix of local-local, smeared-local, local-smeared and smeared-smeared correlators vs the Euclidean time separation in lattice units. Here $\beta = 1.95$, $a\mu_\ell = 0.0035$ on lattice volume $V/a^4 = 32^3 \times 64$. The heavy-quark mass is around 2 times the physical charm quark mass, $\mu_c^{\rm phys}$. (b) The decay constant of heavy-light mesons computed using only local interpolating fields (red circles) or including Gaussian smeared sources (blue squares) are plotted vs the heavy-quark mass, ranging from $\mu_c^{\rm phys}$ up to $\sim 3\mu_c^{\rm phys}$.

trajectories have integration length $\tau = 1$. In each ensemble, gauge configurations are saved on one every two trajectories. For each hadronic observable, the autocorrelation has been studied either by computing directly the $\tau_{\rm int}$ or employing the blocking method to estimate the final error; blocking of about 25 measurements is the typical case for our ensembles in order to safely estimate the final statistical error for M_{ps} and f_{ps} in the light sector. Both methods lead to comparable estimates for the final statistical error. Typical values for $\tau_{\rm int} \in [1, 3]$ for M_{ps} and f_{ps} depending on the gauge ensemble. In our analysis, we have used a number of measurements, indicated by N_{cfg} in Table I, for M_{ps} and f_{ps} performed on gauge configurations each of which is separated by about 20 gauge configurations (or equivalently separated by about 40 trajectories with $\tau = 1$) of the original Monte Carlo history. Based on the above findings we are confident that this choice ensures that autocorrelation is highly suppressed. Moreover, we perform our final analysis by applying the blocking method; we consider blocks of 10 measurements for $\beta = 1.90$ and $\beta = 1.95$ and 6 measurements for $\beta = 2.10$.

Statistical errors on pseudoscalar meson masses and pseudoscalar decay constants have been estimated with the jackknife procedure. Autocorrelation is taken into account using the blocking method. Fit cross correlations are kept under control by generating 1000 bootstrap samples for each gauge configuration ensemble. Notice also that the RC computation has been performed on separate (i.e. totally uncorrelated to the $N_f = 2 + 1 + 1$ sets) $N_f = 4$ gauge configuration ensembles (for details, see Appendix A of Ref. [26]). Moreover, from the comparison of results obtained at the same lattice spacing ($\beta = 1.90$) and light quark mass ($\mu_{\rm sea} = 0.0040$) but on different lattice volumes ($24^3 \times 48$ and $32^3 \times 64$) we notice no significant finite volume effects on the values of all observables relevant for this study. Note that finite size effects are expected to be maximal correspondingly to the $L = 24$, $\mu_\ell = 0.0040$ ensemble as it has the smallest value of $(M_{ps}L)$ among those we have considered (see Ref. [26]).

III. ANALYSIS AND RESULTS

For the determination of the B-physics quantities, we have used the ratio method already applied in the $N_f = 2$ framework [7–9]. The main idea can be summarized in three steps. The first one is the calculation of the values of the observables of interest at heavy quark masses around the charm scale, for which relativistic simulations are reliable (i.e. they produce results with well-controlled discretization errors). The second step consists in evaluating appropriate ratios of the observables at increasing values of the heavy quark mass up to a scale of 2–3 times the charm quark mass (i.e. around 3 GeV). The key point is that the static limit of the measured ratios is exactly known from HQET arguments. The final step of the computation consists in smoothly interpolating data from the charm region to the infinite mass point and extracting their values at the b-mass.

The great computational advantage of this method is that one is able to make B-physics computations using the same relativistic action setup with which the lighter quark computations are performed. Moreover, an extra simulation at the static point limit is not necessary, while the relevant exact information about it is incorporated in the construction of the ratios of observables.

It should be stressed that the use of ratios of observables drastically reduces the discretization errors and at the same time leads to a great suppression of the uncertainties that

come from the QCD matching to HQET. Furthermore the impact of possible (residual) effects of both types of systematic uncertainty on the final results can be controlled by employing appropriate variants of the ratio definition (see below).

First preliminary analyses for the decay constants and the b-quark mass with $N_f = 2+1+1$ gauge ensembles have been presented in Refs. [35,36], respectively.

In the following sections, we present our B-physics analysis where we have made use of improved variants of the ratio method that allow for better control over three main sources of systematic uncertainty, namely, those due to discretization, lattice scale determination and the fitting procedure related to the b-point interpolation.

A. Bottom quark mass and bottom to charm/strange quark mass ratios

At each value of the lattice spacing and sea quark mass ensemble, we build the quantity

$$Q_m \equiv \frac{M_{hs}}{(M_{h\ell})^{\gamma}(M_{cs})^{(1-\gamma)}}, \tag{6}$$

where M_{hs} and $M_{h\ell}$ are the heavy-strange and heavy-light pseudoscalar masses, respectively, while we denote by M_{cs} the mass of the pseudoscalar meson made out of a charm and a strange quark. The parameter γ, not subject to tuning, may take values, typically, in the interval [0, 1). We note that by employing the dimensionless quantity $Q_m(\bar{\mu}_h)$ of Eq. (6) in our analysis, we gain large cancellations of the lattice scale systematics on m_b. Using HQET arguments we know that the asymptotic behavior will be given by

$$\lim_{\mu_h^{\rm pole}\to\infty}\left(\frac{M_{hs}/(M_{h\ell})^{\gamma}}{(\mu_h^{\rm pole})^{(1-\gamma)}}\right) = \text{const}, \tag{7}$$

where $\mu_h^{\rm pole}$ is the heavy quark pole mass. We then consider a sequence of heavy quark masses[1] such that any two successive masses have a common and fixed ratio i.e. $\bar{\mu}_h^{(n)} = \lambda\bar{\mu}_h^{(n-1)}$, $n = 2, 3, \ldots$. The next step is to construct at each value of the sea quark mass and lattice spacing the following ratios:

$$\begin{aligned} &y_Q(\bar{\mu}_h^{(n)}, \lambda; \bar{\mu}_\ell, \bar{\mu}_s, a) \\ &\quad\equiv \frac{Q_m(\bar{\mu}_h^{(n)}; \bar{\mu}_\ell, \bar{\mu}_s, a)}{Q_m(\bar{\mu}_h^{(n-1)}; \bar{\mu}_\ell, \bar{\mu}_s, a)} \cdot \left(\frac{\bar{\mu}_h^{(n)}\rho(\bar{\mu}_h^{(n)}, \mu)}{\bar{\mu}_h^{(n-1)}\rho(\bar{\mu}_h^{(n-1)}, \mu)}\right)^{(\gamma-1)} \\ &\quad= \lambda^{(\gamma-1)}\frac{Q_m(\bar{\mu}_h^{(n)}; \bar{\mu}_\ell, \bar{\mu}_s, a)}{Q_m(\bar{\mu}_h^{(n)}/\lambda; \bar{\mu}_\ell, \bar{\mu}_s, a)}\left(\frac{\rho(\bar{\mu}_h^{(n)}, \mu)}{\rho(\bar{\mu}_h^{(n)}/\lambda, \mu)}\right)^{(\gamma-1)} \end{aligned} \tag{8}$$

with $n = 2, 3, \ldots$ and we have used the relation $\mu_h^{\rm pole} = \rho(\bar{\mu}_h, \mu)\bar{\mu}_h(\mu)$ between the $\overline{\rm MS}$ renormalized quark mass (at the scale μ) and the pole quark mass. The factors ρ's are known perturbatively up to N^{3}LO [37–41]. For each pair of heavy quark masses, we then carry out a simultaneous chiral and continuum fit of the quantity defined in Eq. (8) to obtain $y_Q(\bar{\mu}_h) \equiv y_Q(\bar{\mu}_h, \lambda; \bar{\mu}_{u/d}, \bar{\mu}_s, a = 0)$. By construction this quantity involves (double) ratios of pseudoscalar meson masses at successive values of the heavy quark mass, so we expect that systematic uncertainties due to the use of the perturbative factors $\rho(\bar{\mu}_h, \mu)$ as well as discretization errors will be quite suppressed.[2] In fact, this is the case even for the largest values of the heavy quark mass used in this work, as can be seen in the plot of Fig. 2(a). In Fig. 2(b), the scaling behavior of the ratios is shown at some intermediate value of heavy quark mass pair. Since in the quark mass ratios of Eq. (8) we have taken account of the matching of QCD onto HQET, our ratio $y_Q(\bar{\mu}_h)$ has been defined such that the following *Ansatz* is sufficient to describe the $\bar{\mu}_h$-dependence of y_Q[3]

$$y_Q(\bar{\mu}_h) = 1 + \frac{\eta_1}{\bar{\mu}_h} + \frac{\eta_2}{\bar{\mu}_h^2}. \tag{9}$$

In Eq. (9), the constraint $\lim_{\bar{\mu}_h\to\infty} y_Q(\bar{\mu}_h) = 1$ has already been incorporated. This fit is illustrated in Fig. 3(a). Finally, we compute the b-quark mass through the chain equation,

$$\begin{aligned} &y_Q(\bar{\mu}_h^{(2)})y_Q(\bar{\mu}_h^{(3)})\ldots y_Q(\bar{\mu}_h^{(K+1)}) \\ &\quad= \lambda^{K(\gamma-1)}\frac{Q_m(\bar{\mu}_h^{(K+1)})}{Q_m(\bar{\mu}_h^{(1)})}\cdot\left(\frac{\rho(\bar{\mu}_h^{(K+1)}, \mu)}{\rho(\bar{\mu}_h^{(1)}, \mu)}\right)^{\gamma-1}, \end{aligned} \tag{10}$$

in which the values of the factors in the lhs are evaluated using the result of the fit function [viz. Eq. (9)]. The parameters λ, K (integer) and $\bar{\mu}_h^{(1)}$ are such that $Q_m(\bar{\mu}_h^{(K+1)})$ matches $(M_{Bs}/(M_B)^{\gamma})(M_{Ds})^{(\gamma-1)}$, where $M_{Bs} = 5366.7(4)$ MeV, $M_B = 5279.3(3)$ MeV and $M_{Ds} = 1969.0(1.4)$ MeV are the experimental values of the B_s, B and D_s meson masses [42], respectively. Moreover, $Q_m(\bar{\mu}_h^{(1)})$ (the so-called "triggering point" of the chain equation) can be safely computed in the continuum limit and at the physical pion mass for any value of $\bar{\mu}_h^{(1)}$ chosen in the region of the charm quark mass; see Fig. 3(b). The combined chiral and continuum fit *Ansatz* we used is linear in $\bar{\mu}_\ell$ [43] and in a^2.

[1] In the present analysis, quark masses are expressed in the $\overline{\rm MS}$-scheme at the scale of $\mu = 2$ GeV.

[2] Notice that $M_{cs}^{(1-\gamma)}$ cancels out in the ratios defined in Eq. (8). The dependence on the scale μ in the determination of the factors $\rho(\bar{\mu}_h, \mu)$ is also canceled out in the ratios.

[3] For more details on this point, see Appendix of Ref. [8].

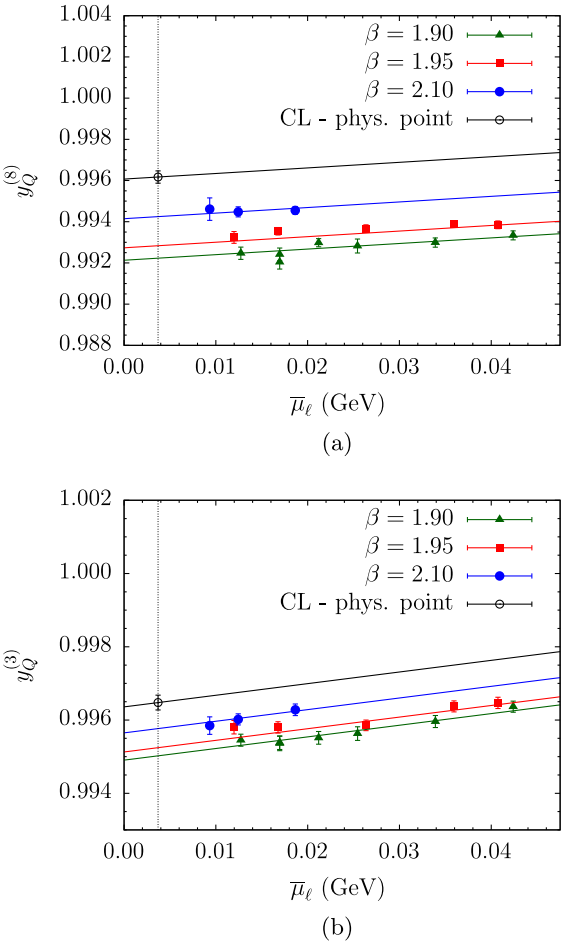

FIG. 2. Combined chiral and continuum fit of the ratio defined in Eq. (8) against the renormalized light quark mass $\bar{\mu}_\ell = \bar{\mu}_{\rm sea}$: (a) for the two largest values of heavy quark mass and (b) for intermediate values of heavy quark masses. The fit *Ansatz* is linear both in $\bar{\mu}_\ell$ and in a^2. The empty black circle is our result at the physical u/d quark mass point in the continuum limit.

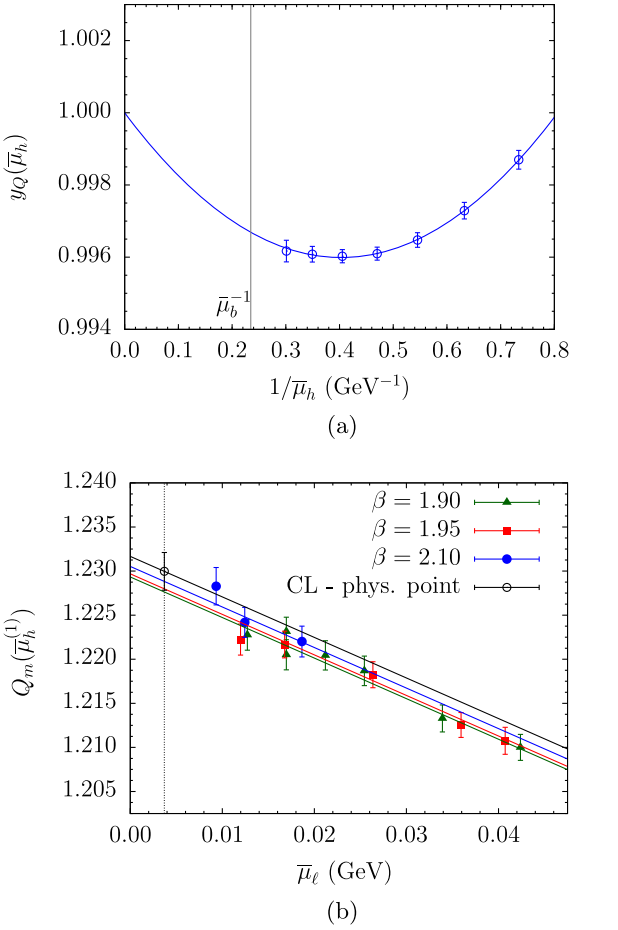

FIG. 3. (a) $y_Q(\bar{\mu}_h)$ against $1/\bar{\mu}_h$ using the fit *Ansatz* of Eq. (9). The vertical black thin line marks the position of $1/\bar{\mu}_b$. (b) Combined chiral and continuum fit at the triggering point, i.e. for the quantity $Q_m(\bar{\mu}_h^{(1)})$ against the renormalized light quark mass $\bar{\mu}_\ell$. The empty black circle is our result at the physical u/d quark mass point in the continuum limit.

The result for the b-quark mass will be given by[4] $\bar{\mu}_b = \lambda^K \bar{\mu}_h^{(1)}$. Figures 2 and 3 refer to one of the analyses we have performed in this work where, by setting, $\bar{\mu}_h^{(1)} = 1.175$ GeV and $\gamma = 0.75$, we find $(\lambda, K) = (1.160, 10)$. We note here that for the running coupling entering in the $\rho(\bar{\mu}_h, \mu)$ function we have used $\Lambda_{\rm QCD}^{N_f=4} = 297(8)$ MeV [42].

A detailed error budget is given in Table II. The description of the various entries follows:

(i) "stat + fit": we gather the error coming from the statistical uncertainties of correlators, the interpolation/extrapolation of the simulated quark masses to the physical values, the extrapolation to the continuum limit, as well as the statistical uncertainties of the RCs. We here recall that statistical errors have been evaluated using the jackknife method and fit cross correlations are taken into account by generating bootstrap samples for each gauge configuration ensemble.

(ii) "syst. discr.": it refers to two sources of systematic uncertainty, both due to cutoff effects. The first is related to the two evaluations of the quark mass RC,

TABLE II. Full error budget for m_b and m_b/m_c.

Uncertainty (in %)	m_b	m_b/m_c
stat + fit	0.9	0.7
syst. discr.	1.6	0.9
syst. ratios	0.8	0.8
syst. chiral	0.4	0.3
syst. trig. point	...	1.2
RI′-$\overline{\rm MS}$ matching	1.3	...
Total	2.4	1.9

[4]Here the value for the b-quark mass is expressed in the $\overline{\rm MS}$-scheme at the scale of 2 GeV, i.e., the same scheme and scale we have decided to work in this analysis.

called M1- and M2-type, which correspond to different ways in which the cutoff effects are treated in the RI-MOM calculation (see Appendix A of Ref. [26]). This amounts to about 1.4%. The second one is the difference (of about 0.8%) between the result obtained through an analysis where data from the coarsest lattice spacing ($\beta = 1.90$) have been excluded and the one that uses data from all three values of β. The two above systematic uncertainties have been added in quadrature.

(iii) "syst. ratios": we collect five different types of systematic uncertainties added in quadrature: (a) systematic uncertainty, of about 0.7%, due to the choice of the parameter γ. In our analysis, we have employed the following values for the parameter $\gamma = 0.0, 0.25, 0.50, 0.60, 0.75, 0.90$; (b) uncertainty in tuning the value of the step λ to satisfy the chain equation (of about 0.3%); (c) in our analysis we have made use of the NLL order formulae for the ρ's while the use of LL or TL ones, thanks to the fact that we work with ratios, would lead to a discrepancy of about 0.3% in the final results; (d) uncertainty of less than 0.1% on the final result if we add to the fit *Ansatz* of Eq. (9) an extra cubic term in $1/\mu_h$; (e) difference of the final result with the one obtained by excluding from the analysis the ratio corresponding to the heaviest quark mass pair (less than 0.1%). Let us stress that the freedom of varying the value of the parameter $\gamma \in [0, 0.9]$ in our analysis,[5] at the cost of a moderate increase of the systematic error in the final value, allows to gain confidence in estimating the systematic uncertainties due to discretization effects and the use of the fit *Ansatz* given in Eq. (9).

(iv) "syst. chiral": it refers to the systematic uncertainty stemming from chiral extrapolation, which is estimated as the spread between the result obtained from all data and the one computed using data with pion mass smaller than 350 MeV.

(v) "RI′-$\overline{\text{MS}}$ matching": for this systematic error estimate, concerning the matching between the two schemes at the typical scales the RCs are computed, we refer the reader to Appendix A of Ref. [26].

The (small) experimental error (of about 0.01% or less) on the values of the $B_{(s)}$ and D_s pseudoscalar meson masses has a negligible impact on our error budget.

Our final result for the b-quark mass is given by the average over the estimates obtained by varying the parameter $\gamma \in [0, 0.9]$ and using M1- or M2-type quark mass RC. The maximum half-difference between extreme values related to the investigation for each one of the sources of systematic error is taken as our estimate of the corresponding systematic uncertainty. Systematic uncertainties are always added in quadrature. Finally, we get

$$m_b(\overline{\text{MS}}, m_b) = 4.26(3)_{\text{stat+fit}}(10)_{\text{syst}}[10]\ \text{GeV}, \tag{11}$$

where the total error (in brackets) is the sum in quadrature of the statistical and the systematic ones.

1. Computation of m_b/m_c and m_b/m_s

The ratio method offers the advantage of determining the ratio m_b/m_c in a simple and fully nonperturbative way. To this end we have to set the triggering point quark mass equal to the physical value of the charm quark mass, $\bar{\mu}_h^{(1)} = \bar{\mu}_c$. We then apply the ratio method employing the following quantity:

$$\hat{Q}_m = \frac{M_{hs}}{(M_{h\ell})^\gamma}, \tag{12}$$

which, unlike the one defined in Eq. (6), must be chosen dimensionful for ensuring charm scale dependence at the triggering point. So by implementing a similar procedure to the case of the b-quark mass, it becomes possible to compute the b to c quark mass ratio directly from the relationship $\bar{\mu}_b = \lambda^K \bar{\mu}_c$. The error budget is also given in Table II. The various entries have a description similar to those for m_b. However there is an extra contribution under the name "syst. trig. point," which refers to the systematic uncertainty related to residual uncertainties in the computation of the (dimensionful) quantity $\hat{Q}_m$ at the triggering point. These uncertainties are not related (directly) to the scale setting and to the renormalization constant's uncertainties that in the bottom to charm quark mass ratio clearly cancel out. They include, instead, the following systematic uncertainties related to the determination of m_c (see Ref. [26]) which refer to the two choices of scaling variable in that fit analysis, the systematic chiral and discretisation uncertainties, the systematic uncertainty stemming from the matching to M_D and M_{Ds} as well as statistical uncertainties in the pseudoscalar mass values computed in the charm region. We consider the sum in quadrature of the above uncertainties to get our estimate.

Our final result reads

$$m_b/m_c = 4.42(3)_{\text{stat+fit}}(8)_{\text{syst}}[8], \tag{13}$$

where the total error (in brackets) is the sum in quadrature of the statistical and systematic ones. As stated above in the quark mass ratio computation, the uncertainties due to the RC and renormalization scheme as well as the systematic lattice scale uncertainties cancel out.

Finally, by combining the result of Eq. (13) with the result

$$m_c/m_s = 11.62(16)_{\text{stat+fit}}(1)_{\text{syst}}[16] \tag{14}$$

[5]Notice that in practice for $\gamma \in (0.9, 1.0)$ it becomes difficult to estimate the systematic uncertainty in the tuning of λ from the chain equation (10).

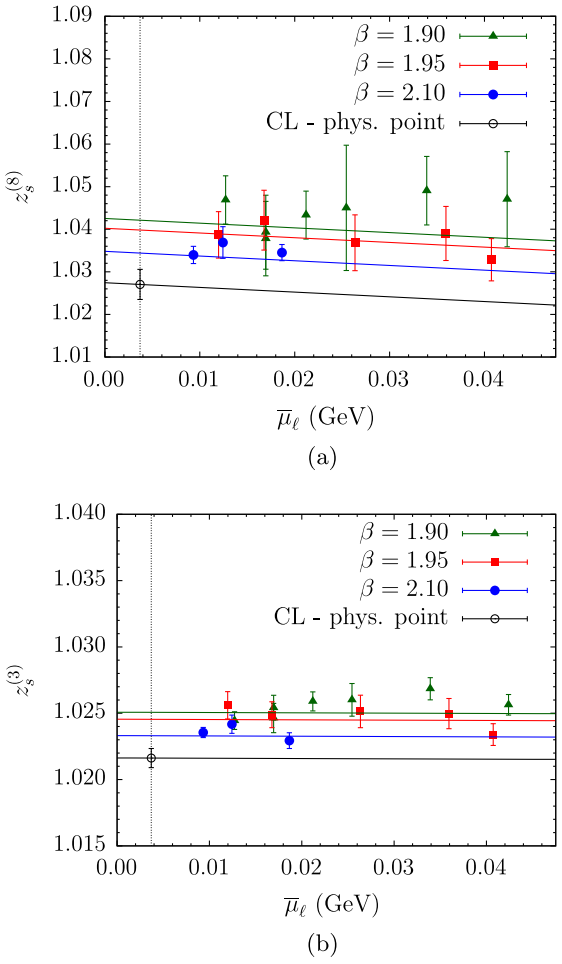

FIG. 4. Combined chiral and continuum fit for the ratio z_s against $\bar{\mu}_\ell$ calculated: (a) between the two largest heavy quark mass values used in this work; (b) for intermediate values of the heavy quark masses. The empty black circle is our result at the physical u/d quark mass point in the continuum limit.

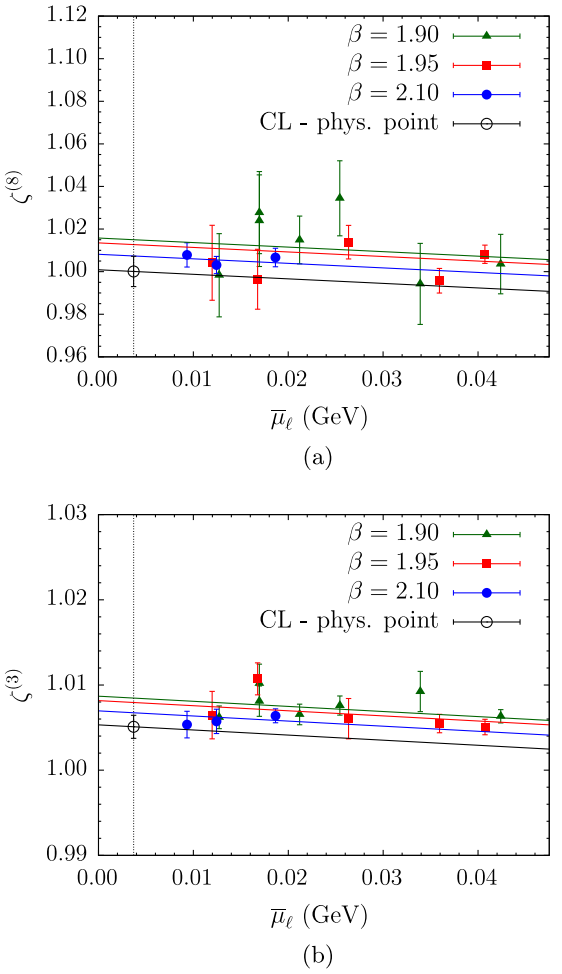

FIG. 5. Same as in Fig. 4 for the ratio ζ.

presented in Ref. [26], we obtain the value for the bottom to strange quark mass ratio,

$$m_b/m_s = 51.4(1.1)_{\text{stat+fit}}(0.9)_{\text{syst}}[1.4], \qquad (15)$$

where, again, the sum of the statistical and the systematic errors in quadrature give the total error (in brackets). The error estimate has been obtained assuming full correlation between the "stat + fit" uncertainties of Eqs. (13) and (14), which thus have been added linearly, whereas systematic uncertainties have been added in quadrature. Our result of Eq. (15) compares well with the (nonperturbative) result $m_b/m_s = 52.55(55)$ obtained by the HPQCD Collaboration [44]. It is also in agreement with the Georgi-Jarlskog prediction [45] that, for certain classes of grand unified theories, the ratio of b to s quark masses should be equal to $3m_\tau/m_\mu = 50.45$.

B. *B*-pseudoscalar decay constants

At each value of the lattice spacing and sea quark mass ensemble, we evaluate the quantity

$$\mathcal{F}_{hq} \equiv f_{hq}/M_{hq}, \qquad q = \ell, s, \qquad (16)$$

for which the appropriate HQET asymptotic conditions lead to

$$\lim_{\mu_h^{\text{pole}} \to \infty} \mathcal{F}_{hq}(\mu_h^{\text{pole}})^{3/2} = \text{const.} \qquad (17)$$

and

$$\lim_{\mu_h^{\text{pole}} \to \infty} (\mathcal{F}_{hs}/\mathcal{F}_{h\ell}) = \text{const.} \qquad (18)$$

Based on QCD to HQET matching of heavy-light meson decay constant and quark mass, we define the ratios

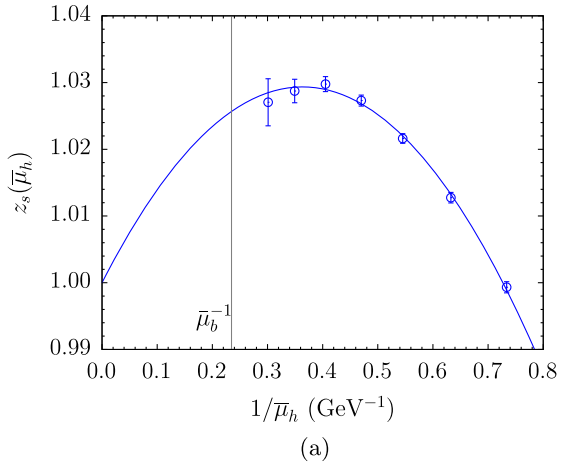

(a)

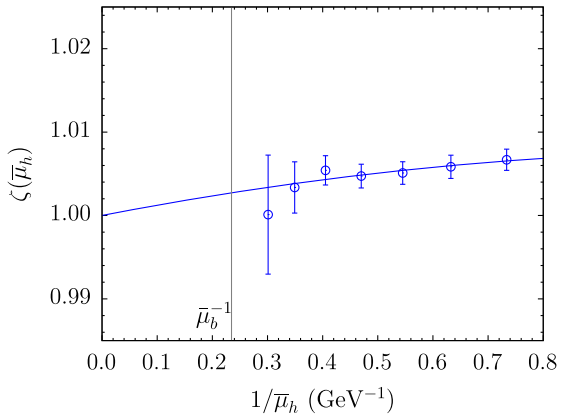

(b)

FIG. 6. Fit of $z_s(\bar{\mu}_h)$ (top panel) and $\zeta(\bar{\mu}_h)$ (bottom panel) against $1/\bar{\mu}_h$. The fit function in both panels has a polynomial form of the type given in Eq. (9). The vertical black thin line marks the position of $1/\bar{\mu}_b$.

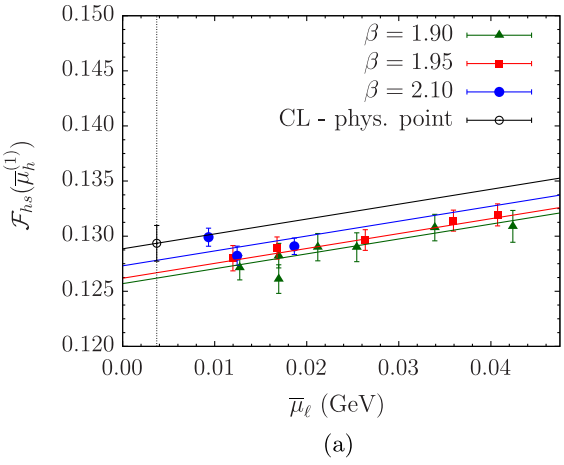

(a)

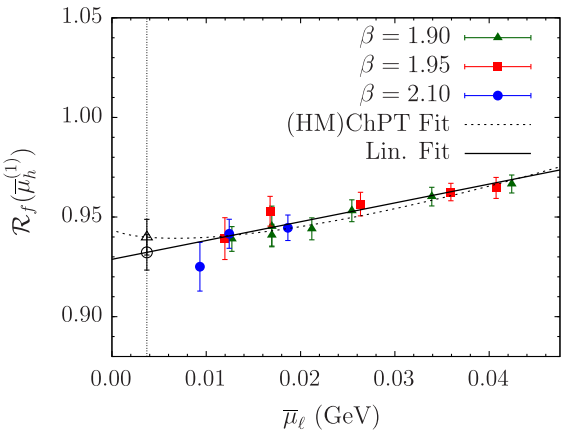

(b)

FIG. 7. Combined chiral and continuum fit against $\bar{\mu}_\ell$: (a) linear fit in $\bar{\mu}_\ell$ and in a^2 for the triggering point of $\mathcal{F}(\bar{\mu}_h^{(1)})$; (b) fit *Ansätze* for $\mathcal{R}_f(\bar{\mu}_h^{(1)})$ given in Eqs. (25) and (26). The empty black symbols denote results at the physical u/d quark mass point in the continuum limit.

$$z_s(\bar{\mu}_h, \lambda; \bar{\mu}_s, a) = \lambda^{3/2} \frac{\mathcal{F}_{hs}(\bar{\mu}_h, \bar{\mu}_s, a)}{\mathcal{F}_{hs}(\bar{\mu}_h/\lambda, \bar{\mu}_s, a)} \cdot \frac{C_A^{\rm stat}(\mu^*, \bar{\mu}_h/\lambda)}{C_A^{\rm stat}(\mu^*, \bar{\mu}_h)} \frac{[\rho(\bar{\mu}_h, \mu)]^{3/2}}{[\rho(\bar{\mu}_h/\lambda, \mu)]^{3/2}} \tag{19}$$

$$z_d(\bar{\mu}_h, \lambda; \bar{\mu}_\ell, a) = \lambda^{3/2} \frac{\mathcal{F}_{h\ell}(\bar{\mu}_h, \bar{\mu}_\ell, a)}{\mathcal{F}_{h\ell}(\bar{\mu}_h/\lambda, \bar{\mu}_\ell, a)} \cdot \frac{C_A^{\rm stat}(\mu^*, \bar{\mu}_h/\lambda)}{C_A^{\rm stat}(\mu^*, \bar{\mu}_h)} \frac{[\rho(\bar{\mu}_h, \mu)]^{3/2}}{[\rho(\bar{\mu}_h/\lambda, \mu)]^{3/2}}. \tag{20}$$

The factor $C_A^{\rm stat}(\mu^*, \bar{\mu}_h)$ is known up to N^{2}LO in PT [46]. It provides the matching between the $(h\ell)$ decay constant in QCD and its static-light counterpart in HQET.[6] For the calculation of the decay constant ratio, we also form the double ratio:

$$\zeta(\bar{\mu}_h, \lambda; \bar{\mu}_\ell, \bar{\mu}_s, a) = \frac{z_s(\bar{\mu}_h, \lambda; \bar{\mu}_s, a)}{z_d(\bar{\mu}_h, \lambda; \bar{\mu}_\ell, a)}. \tag{21}$$

The ratios z_d, z_s and ζ have, by construction, an exactly known static limit equal to unity. They also show smooth chiral and continuum combined behavior. This is a consequence of the fact that z_d, z_s and ζ (as it is also the case for the y ratios) are simply ratios of quantities evaluated at nearby values of the heavy quark mass for which discretization errors get suppressed. Figures 4(a) and 5(a) are two examples illustrating the quality of the combined chiral and continuum fits for z_s and ζ respectively, at the largest heavy quark mass values used in the decay constant analysis. See also the analogous Figs. 4(b) and 5(b) for the same quantities at intermediate values of the heavy quark mass pair. Notice that, since the cutoff effects for the ratios are under good control, even for rather large values of the heavy quark mass pairs the combined chiral and continuum fits of ratios are reliable.

[6]Notice that the renormalization scale μ^* of HQET as well as the quark mass renormalization scale μ cancel when ratios are considered.

TABLE III. Full error budget for f_{Bs}, f_{Bs}/f_B and f_B.

Uncertainty (in %)	f_{Bs}	f_{Bs}/f_B	f_B
stat + fit	1.7	1.5	2.5
syst. discr.	1.3	0.6	0.7
syst. ratios	0.5	0.3	0.6
syst. chiral	0.3	0.2	0.4
syst. trig. point & f_K/f_π	⋯	1.3	1.3
Total	2.2	2.1	3.0

In Figs. 6(a) and 6(b), we show the dependence of $z_s(\bar{\mu}_h)$ and $\zeta(\bar{\mu}_h)$ on the inverse heavy quark mass, respectively. The fit *Ansätze* we have used are polynomial fit functions in the inverse heavy quark mass analogous to the one displayed in Eq. (9). For the case of the double ratio $\zeta(\bar{\mu}_h)$, we have also tried a linear fit in $1/\bar{\mu}_h$ where the exact condition $\lim_{\bar{\mu}_h\to\infty}\zeta(\bar{\mu}_h)=1$ is explicitly implemented.

In order to determine f_{Bs} and f_{Bs}/f_B, we exploit the equations

$$\begin{aligned} &z_s(\bar{\mu}_h^{(2)})z_s(\bar{\mu}_h^{(3)})\ldots z_s(\bar{\mu}_h^{(K+1)}) \\ &\quad=\lambda^{3K/2}\frac{\mathcal{F}_{hs}(\bar{\mu}_h^{(K+1)})}{\mathcal{F}_{hs}(\bar{\mu}_h^{(1)})}\cdot\frac{C_A^{\rm stat}(\mu^*,\bar{\mu}_h^{(1)})}{C_A^{\rm stat}(\mu^*,\bar{\mu}_h^{(K+1)})} \\ &\quad\times\left(\frac{\rho(\bar{\mu}_h^{(K+1)},\mu)}{\rho(\bar{\mu}_h^{(1)},\mu)}\right)^{3/2}, \end{aligned} \tag{22}$$

$$\begin{aligned} &\zeta(\bar{\mu}_h^{(2)})\zeta(\bar{\mu}_h^{(3)})\ldots\zeta(\bar{\mu}_h^{(K+1)}) \\ &\quad=\left(\frac{\mathcal{F}_{hs}(\bar{\mu}_h^{(K+1)})/\mathcal{F}_{hu/d}(\bar{\mu}_h^{(K+1)})}{\mathcal{F}_{hs}(\bar{\mu}_h^{(1)})/\mathcal{F}_{hu/d}(\bar{\mu}_h^{(1)})}\right). \end{aligned} \tag{23}$$

The values of the left-hand sides of the above equations are taken from the fits of Figs. 6(a) and 6(b), respectively. Setting $\bar{\mu}_h^{(K+1)}=\bar{\mu}_b$ and having determined the values of $\mathcal{F}_{hs}(\bar{\mu}_h^{(1)})$ and $[\mathcal{F}_{hs}(\bar{\mu}_h^{(1)})/\mathcal{F}_{hu/d}(\bar{\mu}_h^{(1)})]$ from a combined chiral and continuum fit, and using experimental input for the B_s and B-meson masses, we finally obtain our results for f_{Bs} and (f_{Bs}/f_B). The use of the observable of Eq. (16) yields the continuum limit determination of f_{Bs} in physical units via the experimental value of M_{Bs}, leading thus to the elimination of the lattice scale systematic uncertainty. As for the combined chiral and continuum fit of the triggering point quantity $\mathcal{F}_{hs}(\bar{\mu}_h^{(1)})$, this poses no problems because $\mathcal{F}_{hs}(\bar{\mu}_h^{(1)})$ exhibits only tolerably small cutoff effects and very weak dependence on the light quark mass [see Fig. 7(a)].

In order to estimate the triggering point ratio $[\mathcal{F}_{hs}(\bar{\mu}_h^{(1)})/\mathcal{F}_{hu/d}(\bar{\mu}_h^{(1)})]$, we build the following double ratio,

$$\mathcal{R}_f=[(\mathcal{F}_{hs}/\mathcal{F}_{h\ell})/(f_{s\ell}/f_{\ell\ell})], \tag{24}$$

which provides the advantage of large cancellations in the chiral logarithmic terms [47,48]. One then can get the desired triggering point ratio by combining the continuum limit result for $\mathcal{R}_f$ with the analogous result for the ratio of the K to π decay constants, (f_K/f_π). In Fig. 7(b), we present the combined continuum and chiral extrapolation for $\mathcal{R}_f$. We have used two fit *Ansätze*. The first is linear in

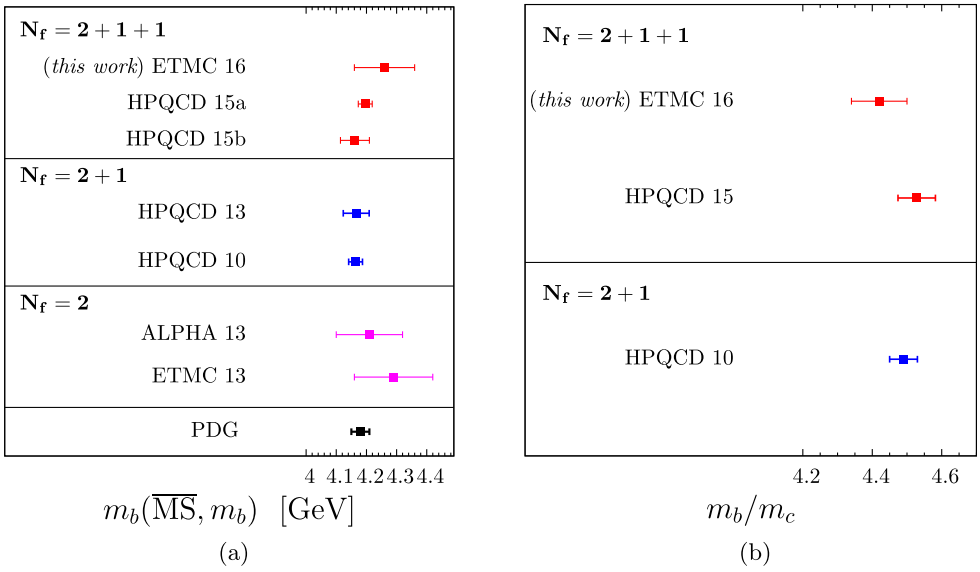

FIG. 8. A comparison of the available continuum extrapolated lattice determinations for m_b, panel (a), and m_b/m_c, panel (b). For the other results, we refer to (from top to bottom) (a) Refs. [44,50,51,52,53,9,42]; (b) Refs. [44,52].

$\bar{\mu}_\ell$ while the second one is suggested by the combined use of the SU(2) ChPT and HMChPT. They read

$$\mathcal{R}_f^{(1)} = a_h^{(1)} + b_h^{(1)}\bar{\mu}_\ell + D_h^{(1)}a^2 \tag{25}$$

$$\mathcal{R}_f^{(2)} = a_h^{(2)}\left[1 + b_h^{(2)}\bar{\mu}_\ell + \left[\frac{3(1+3\hat{g}^2)}{4} - \frac{5}{4}\right] \times \frac{2B_0\bar{\mu}_\ell}{(4\pi f_0)^2}\log\left(\frac{2B_0\bar{\mu}_\ell}{(4\pi f_0)^2}\right)\right] + D_h^{(2)}a^2. \tag{26}$$

The magnitude of the logarithmic term in this fit depends on the value of $\hat{g}$. Given the form of Eq. (26) we have used $\hat{g} = 0.61(7)$ [42], since for this value we get the most conservative estimate for the fit systematic uncertainty.

As can be noticed from Fig. 7(b), discretization effects on $\mathcal{R}_f$ are small. Moreover, the two estimates for the triggering point ratio at the physical light quark mass are compatible within less than two standard deviations. So we take their average as our best estimate and we consider their half difference as a systematic uncertainty.

The central values of f_{Bs} and f_{Bs}/f_B have been obtained from the weighted average over the various estimates corresponding to the sets of values $(\bar{\mu}_h^{(1)}, \lambda, K, \gamma)$ employed

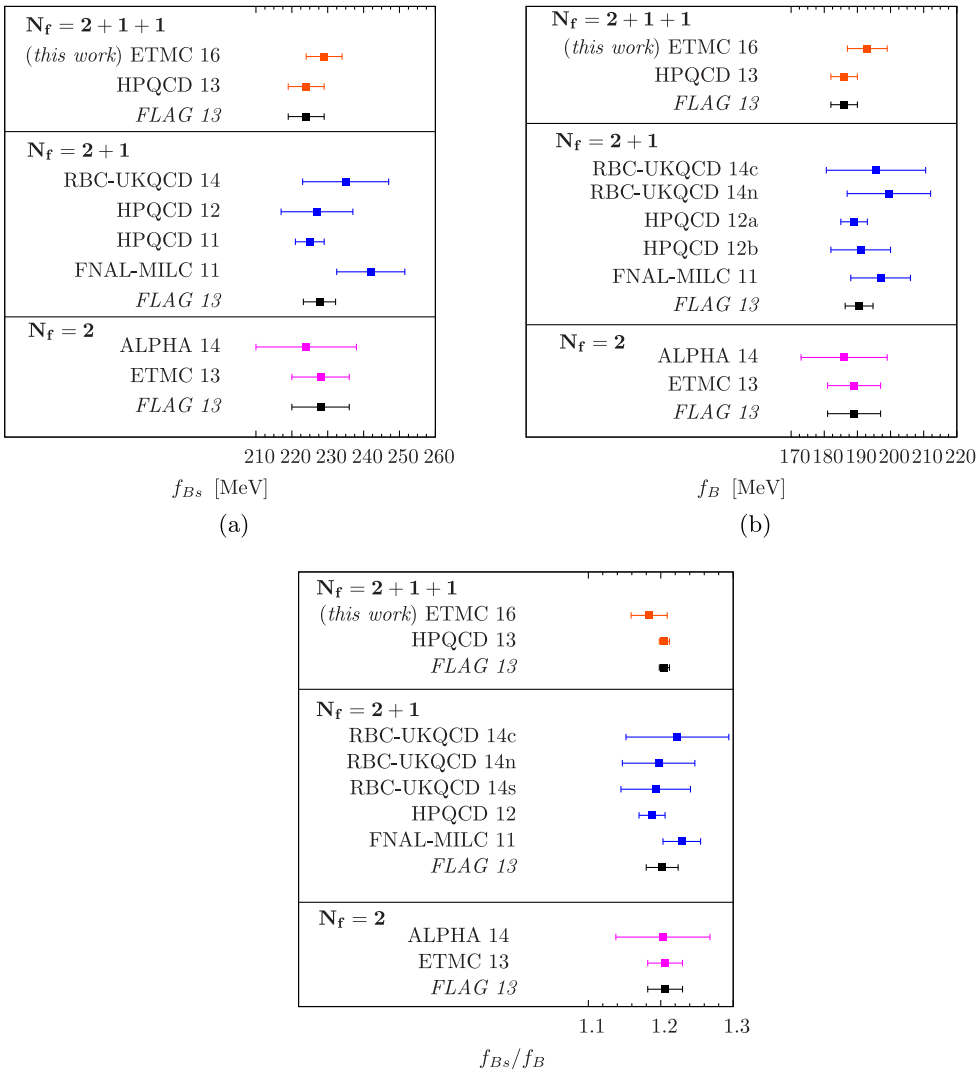

FIG. 9. A comparison of the available continuum extrapolated lattice determinations for (a) f_{Bs}, (b) f_B and (c) f_{Bs}/f_B. For results by other groups, we refer to (from top to bottom) (a) Refs. [54,10,55,56,57,58,10,59,9,10] *FLAG 13* estimates are determined by HPQCD 13 for $N_f = 2+1+1$, HPQCD 12, HPQCD 11 and FNAL-MILC 11 for $N_f = 2+1$ and ETMC 13 for $N_f = 2$; (b) Refs. [54,10,55,55,56,56,58,10,59,9,10] *FLAG 13* estimates are determined by HPQCD 13 for $N_f = 2+1+1$, HPQCD 12a, HPQCD 12b and FNAL-MILC 11 for $N_f = 2+1$ and ETMC 13 for $N_f = 2$; (c) Refs. [54,10,55,55,60,56,58,10,59,9,10] *FLAG 13* estimates are determined by HPQCD 13 for $N_f = 2+1+1$, HPQCD 12a and FNAL-MILC 11 for $N_f = 2+1$ and ETMC 13 for $N_f = 2$. Results for f_{Bs} and f_B from Ref. [60] display somewhat bigger errors than the results shown above, so we have not included them in the plots.

in our b-quark mass analysis. The f_B computation is carried out through the expression $f_B = f_{Bs}/(f_{Bs}/f_B)$. We now give the description of the full error budget for the decay constants, presented in Table III:

(i) "stat + fit": this has been estimated along the same lines as for the b-quark mass.

(ii) "syst. discr.": it includes two sources of systematic discretization errors, then added in quadrature. Concerning the first one we take into account the fact that for the decay constants computation at the b-quark point we have collected as many estimates as there are the respective sets $(\bar{\mu}_h^{(1)}, \lambda, K, \gamma)$ employed in our b-mass analysis. We then consider the maximum spread of these results from their average (about 0.5% for f_{Bs} and 0.4% for f_{Bs}/f_B). The second systematic error related to cutoff effects has been estimated by investigating the impact of removing from our analysis the coarsest lattice ($\beta = 1.90$) data. The maximum difference between results from the full data analysis and the one when only data from the two finest lattices are used amounts to 1.2% for f_{Bs} and 0.4% for f_{Bs}/f_B.

(iii) "syst. ratios": we have checked the impact on our final results of the various sources of systematic uncertainty related to the ratio analysis. We have worked along the same lines as for the b-mass error budget. In particular, we have checked the effects by (a) varying the polynomial fit *Ansatz* used for interpolating to the b-quark mass, (b) excluding the heaviest quark mass pair from our analysis and (c) changing the perturbative order for the ρ's and $C_A^{\rm stat}$ from NLL to LL. None of these tests gave a change to the values of f_{Bs} and f_{Bs}/f_B larger than 0.3–0.4%. The final estimates in Table III correspond to the sum in quadrature of the individual spreads due to (a), (b) and (c).

(iv) "syst. chiral": we estimate the systematic uncertainty due to chiral extrapolation from the difference between results obtained from all data or using only data corresponding to pion mass less than 350 MeV.

(v) "syst. trig. point & f_K/f_π": this concerns only f_{Bs}/f_B and f_B and it is given as the sum in quadrature of the chiral extrapolation systematic uncertainty, which we estimate from the spread of results obtained from the two-fit *Ansätze* of Eqs. (25) and (26) (of about 0.4%), and the error in the determination of f_K/f_π; for the latter we have used the value $f_K/f_\pi = 1.188(15)$ from Ref. [49].

Our final results for the decay constants read

$$f_{Bs} = 229(4)_{\rm stat+fit}(3)_{\rm syst}[5]\ \text{MeV}, \tag{27}$$

$$f_{Bs}/f_B = 1.184(18)_{\rm stat+fit}(18)_{\rm syst}[25], \tag{28}$$

$$f_B = 193(5)_{\rm stat+fit}(3)_{\rm syst}[6]\ \text{MeV}, \tag{29}$$

$$(f_{Bs}/f_B)/(f_K/f_\pi) = 0.997(15)_{\rm stat}(7)_{\rm syst}[17], \tag{30}$$

where the total error (in brackets) is the sum in quadrature of the statistical and the systematic ones.

IV. CONCLUSIONS

Using the ratio method, we have obtained nonperturbative results extrapolated to the continuum limit for the b-quark mass and its ratio to the charm and the strange quark mass. Moreover, we have evaluated in the continuum limit the pseudoscalar B-decay constants, f_{Bs}, f_B and their ratio as well as the (double) ratio of the latter with f_K/f_π. It is worth mentioning that the ratios between the SU(3) breaking ratios $(f_{Bs}/f_B)/(f_K/f_\pi)$ computed in this paper and the one of $(f_{Ds}/f_D)/(f_K/f_\pi) = 1.003(14)$ determined in Ref. [49], are both perfectly compatible with unity within the errors, indicating, thus, an almost negligible dependence on the quark mass. Our results, Eqs. (11), (13), (15) and (27)–(30), are of high precision with well-controlled systematic uncertainties. In Figs. 8 and 9, we compare our results with the ones obtained by other lattice collaborations. Each panel includes determinations of the relevant observable that are carried out in the continuum limit by using unquenched lattice simulations with $N_f = 2, 2+1$ and $2+1+1$ dynamical quarks.

ACKNOWLEDGMENTS

We warmly thank our colleagues of the ETM Collaboration for fruitful discussions. We acknowledge the CPU time provided by the PRACE Research Infrastructure under the Projects No. PRA027 (QCD Simulations for Flavor Physics in the Standard Model and Beyond) and No. PRA067 (First Lattice QCD Study of B-physics with Four Flavors of Dynamical Quarks) on the BG/P and BG/Q systems at the Jülich SuperComputing Center (Germany) and at CINECA (Italy) and by the agreement between INFN and CINECA under the specific initiative INFN-LQCD123 on the Fermi BG/Q system at CINECA (Italy).

[1] A. Djouadi, The anatomy of electro-weak symmetry breaking. I: The Higgs boson in the standard model, Phys. Rep. **457**, 1 (2008).

[2] V. Khachatryan *et al.* (LHCb and CMS Collaborations), Observation of the rare $B_s^0 \to \mu^+\mu^-$ decay from the combined analysis of CMS and LHCb data, Nature (London) **522**, 68 (2015).

[3] I. Adachi *et al.* (Belle Collaboration), Evidence for $B^- \to \tau^-\bar{\nu}_\tau$ with a Hadronic Tagging Method Using the Full Data Sample of Belle, Phys. Rev. Lett. **110**, 131801 (2013).

[4] J. P. Lees *et al.* (*BABAR* Collaboration), Evidence of $B^+ \to \tau^+\nu$ decays with hadronic B tags, Phys. Rev. D **88**, 031102 (2013).

[5] R. Baron, P. Boucaud, J. Carbonell, A. Deuzeman, V. Drach *et al.* (ETM Collaboration), Light hadrons from lattice QCD with light (u,d), strange and charm dynamical quarks, J. High Energy Phys. 06 (2010) 111.

[6] R. Baron *et al.* (ETM Collaboration), Computing K and D meson masses with $N_f = 2 + 1 + 1$ twisted mass lattice QCD, Comput. Phys. Commun. **182**, 299 (2011).

[7] B. Blossier *et al.* (ETM Collaboration), A proposal for B-physics on current lattices, J. High Energy Phys. 04 (2010) 049.

[8] P. Dimopoulos *et al.* (ETM Collaboration), Lattice QCD determination of m_b, f_B and f_{Bs} with twisted mass Wilson fermions, J. High Energy Phys. 01 (2012) 046.

[9] N. Carrasco, M. Ciuchini, P. Dimopoulos, R. Frezzotti, V. Gimenez *et al.* (ETM Collaboration), B-physics from Nf = 2 tmQCD: the Standard Model and beyond, J. High Energy Phys. 03 (2014) 016.

[10] S. Aoki, Y. Aoki, C. Bernard, T. Blum, G. Colangelo *et al.* (FLAG Collaboration), Review of lattice results concerning low-energy particle physics, Eur. Phys. J. C **74**, 2890 (2014).

[11] C. M. Bouchard, Testing the Standard Model under the weight of heavy flavors, *Proc. Sci.*, LATTICE2015 (2015) 002 [arXiv:1501.03204].

[12] C. Pena, Progress and prospects for heavy favour physics on the lattice, in *Proceedings of 33nd International Symposium on Lattice Field Theory (Lattice 2015), Kobe, Japan* (2015).

[13] J. L. Rosner, S. Stone, and R. S. Van de Water, Leptonic decays of charged pseudoscalar mesons—2015, arXiv: 1509.02220.

[14] K. Chetyrkin, J. H. Kuhn, A. Maier, P. Maierhofer, P. Marquard, M. Steinhauser, and C. Sturm, Precise charm- and bottom-quark masses: Theoretical and experimental uncertainties, Theor. Math. Phys. **170**, 217 (2012).

[15] S. Narison, Revisiting f_B and $m_b(m_b)$ from HQET spectral sum rules, Phys. Lett. B **721**, 269 (2013).

[16] W. Lucha, D. Melikhov, and S. Simula, Accurate bottom-quark mass from Borel QCD sum rules for f_B and f_{B_s}, Phys. Rev. D **88**, 056011 (2013).

[17] Y. Iwasaki, Renormalization group analysis of lattice theories and improved lattice action: Two-dimensional nonlinear O(N) sigma model, Nucl. Phys. **B258**, 141 (1985).

[18] Y. Iwasaki, K. Kanaya, T. Kaneko, and T. Yoshie, Scaling in SU(3) pure gauge theory with a renormalization group improved action, Phys. Rev. D **56**, 151 (1997).

[19] R. Frezzotti and G. C. Rossi, Chirally improving Wilson fermions. I: O(a) improvement, J. High Energy Phys. 08 (2004) 007.

[20] R. Frezzotti and G. C. Rossi, Twisted-mass lattice QCD with mass non-degenerate quarks, Nucl. Phys. B, Proc. Suppl. **128**, 193 (2004).

[21] P. Boucaud *et al.* (ETM Collaboration), Dynamical twisted mass fermions with light quarks, Phys. Lett. B **650**, 304 (2007).

[22] P. Boucaud *et al.* (ETM Collaboration), Dynamical twisted mass fermions with light quarks: Simulation and analysis details, Comput. Phys. Commun. **179**, 695 (2008).

[23] R. Baron *et al.* (ETM Collaboration), Light meson physics from maximally twisted mass lattice QCD, J. High Energy Phys. 08 (2010) 097.

[24] K. Osterwalder and E. Seiler, Gauge field theories on the lattice, Ann. Phys. (N.Y.) **110**, 440 (1978).

[25] R. Frezzotti and G. C. Rossi, Chirally improving Wilson fermions. II: Four-quark operators, J. High Energy Phys. 10 (2004) 070.

[26] N. Carrasco *et al.* (ETM Collaboration), Up, down, strange and charm quark masses with $N_f = 2 + 1 + 1$ twisted mass lattice QCD, Nucl. Phys. **B887**, 19 (2014).

[27] R. Frezzotti, P. A. Grassi, S. Sint, and P. Weisz (Alpha Collaboration), Lattice QCD with a chirally twisted mass term, J. High Energy Phys. 08 (2001) 058.

[28] M. Foster and C. Michael (UKQCD Collaboration), Quark mass dependence of hadron masses from lattice QCD, Phys. Rev. D **59**, 074503 (1999).

[29] C. McNeile and C. Michael (UKQCD Collaboration), Decay width of light quark hybrid meson from the lattice, Phys. Rev. D **73**, 074506 (2006).

[30] S. Gusken, A study of smearing techniques for hadron correlation functions, Nucl. Phys. B, Proc. Suppl. **17**, 361 (1990).

[31] M. Albanese *et al.* (APE Collaboration), Glueball masses and string tension in lattice QCD, Phys. Lett. B **192**, 163 (1987).

[32] B. Blossier, M. Della Morte, G. von Hippel, T. Mendes, and R. Sommer, On the generalized eigenvalue method for energies and matrix elements in lattice field theory, J. High Energy Phys. 04 (2009) 094.

[33] R. Frezzotti, G. Martinelli, M. Papinutto, and G. Rossi, Reducing cutoff effects in maximally twisted lattice QCD close to the chiral limit, J. High Energy Phys. 04 (2006) 038.

[34] P. Dimopoulos, R. Frezzotti, C. Michael, G. Rossi, and C. Urbach, O(a^2) cutoff effects in lattice Wilson fermion simulations, Phys. Rev. D **81**, 034509 (2010).

[35] N. Carrasco *et al.* (ETM Collaboration), A $N_f = 2 + 1 + 1$ 'twisted' determination of the b-quark mass, f_B and f_{B_s}, *Proc. Sci.*, LATTICE2013 (2014) 313 [arXiv:1311.2837].

[36] A. Bussone *et al.*, Heavy flavour precision physics from Nf = 2 + 1 + 1 lattice simulations, in *Proceedings of International Conference on High Energy Physics (ICHEP 2014), Valencia, Spain, 2014* (2014).

[37] K. Chetyrkin and A. Retey, Renormalization and running of quark mass and field in the regularization invariant and MS-bar schemes at three loops and four loops, Nucl. Phys. **B583**, 3 (2000).

[38] N. Gray, D. J. Broadhurst, W. Grafe, and K. Schilcher, Three loop relation of quark (modified) MS and pole masses, Z. Phys. C **48**, 673 (1990).
[39] D. J. Broadhurst, N. Gray, and K. Schilcher, Gauge invariant on-shell Z(2) in QED, QCD and the effective field theory of a static quark, Z. Phys. C **52**, 111 (1991).
[40] K. Chetyrkin and M. Steinhauser, Short Distance Mass of a Heavy Quark at Order α_s^3, Phys. Rev. Lett. **83**, 4001 (1999).
[41] K. Melnikov and T. v. Ritbergen, The three loop relation between the MS-bar and the pole quark masses, Phys. Lett. B **482**, 99 (2000).
[42] K. A. Olive *et al.* (Particle Data Group Collaboration), Review of particle physics, Chin. Phys. C **38**, 090001 (2014).
[43] A. Roessl, Pion kaon scattering near the threshold in chiral SU(2) perturbation theory, Nucl. Phys. **B555**, 507 (1999).
[44] B. Chakraborty, C. T. H. Davies, B. Galloway, P. Knecht, J. Koponen, G. Donald, R. Dowdall, G. Lepage, and C. McNeile, High-precision quark masses and QCD coupling from $n_f = 4$ lattice QCD, Phys. Rev. D **91**, 054508 (2015).
[45] H. Georgi and C. Jarlskog, A new lepton-quark mass relation in a unified theory, Phys. Lett. **86B**, 297 (1979).
[46] K. G. Chetyrkin and A. G. Grozin, Three-loop anomalous dimension of the heavy-light quark current in HQET, Nucl. Phys. **B666**, 289 (2003).
[47] D. Becirevic, S. Fajfer, S. Prelovsek, and J. Zupan, Chiral corrections and lattice QCD results for f_{B_s}/f_{B_d} and $\Delta m_{B_s}/\Delta m_{B_d}$, Phys. Lett. B **563**, 150 (2003).
[48] B. Blossier *et al.* (ETM Collaboration), Pseudoscalar decay constants of kaon and D-mesons from $N_f = 2$ twisted mass Lattice QCD, J. High Energy Phys. 07 (2009) 043.
[49] N. Carrasco *et al.* (ETM Collaboration), Leptonic decay constants f_K, f_D, and f_{D_s} with $N_f = 2 + 1 + 1$ twisted-mass lattice QCD, Phys. Rev. D **91**, 054507 (2015).
[50] B. Colquhoun, R. J. Dowdall, C. T. H. Davies, K. Hornbostel, and G. P. Lepage, Υ and Υ' Leptonic Widths, a_μ^b and m_b from full lattice QCD, Phys. Rev. D **91**, 074514 (2015).
[51] A. J. Lee, C. J. Monahan, R. R. Horgan, C. T. H. Davies, R. J. Dowdall, and J. Koponen (HPQCD Collaboration), The mass of the b-quark from lattice NRQCD and lattice perturbation theory, Phys. Rev. D **87**, 074018 (2013).
[52] C. McNeile, C. Davies, E. Follana, K. Hornbostel, and G. Lepage, High-Precision c and b masses, and QCD coupling from current-current correlators in lattice and continuum QCD, Phys. Rev. D **82**, 034512 (2010).
[53] F. Bernardoni *et al.*, The b-quark mass from non-perturbative $N_f = 2$ heavy quark effective theory at $O(1/m_h)$, Phys. Lett. B **730**, 171 (2014).
[54] R. Dowdall, C. Davies, R. Horgan, C. Monahan, and J. Shigemitsu (HPQCD Collaboration), B-Meson Decay Constants from Improved Lattice NRQCD and Physical u, d, s and c Sea Quarks, Phys. Rev. Lett. **110**, 222003 (2013).
[55] N. H. Christ, J. M. Flynn, T. Izubuchi, T. Kawanai, C. Lehner, A. Soni, R. S. Van de Water, and O. Witzel, B-meson decay constants from $2 + 1$-flavor lattice QCD with domain-wall light quarks and relativistic heavy quarks, Phys. Rev. D **91**, 054502 (2015).
[56] H. Na, C. J. Monahan, C. T. H. Davies, R. Horgan, G. Peter Lepage, and J. Shigemitsu, The B and Bs meson decay constants from lattice QCD, Phys. Rev. D **86**, 034506 (2012).
[57] C. McNeile, C. Davies, E. Follana, K. Hornbostel, and G. Lepage, High-precision f_{B_s} and HQET from relativistic lattice QCD, Phys. Rev. D **85**, 031503 (2012).
[58] A. Bazavov *et al.* (Fermilab Lattice and MILC Collaborations), B- and D-meson decay constants from three-flavor lattice QCD, Phys. Rev. D **85**, 114506 (2012).
[59] F. Bernardoni *et al.* (ALPHA Collaboration), Decay constants of B-mesons from non-perturbative HQET with two light dynamical quarks, Phys. Lett. B **735**, 349 (2014).
[60] Y. Aoki, T. Ishikawa, T. Izubuchi, C. Lehner, and A. Soni, Neutral *B* meson mixings and *B* meson decay constants with static heavy and domain-wall light quarks, Phys. Rev. D **91**, 114505 (2015).